Low Cost, Wideband Ultrasonic Transmitter and Receiver for Array Signal Processing Applications

J.R. Gonzalez*, Juan.Gonzalez-Hernandez@ucdconnect.ie
C.J. Bleakley, chris.bleakley@ucd.ie
Complex & Adaptive Systems Laboratory
School of Computer Science and Informatics
University College Dublin
Belfield, Dublin 4, Ireland.

***Abstract*—This paper presents a low cost, wideband ultrasonic transmitter for in-air ultrasonic applications based on a conventional narrowband piezoceramic transducer with a L-R circuit modification. An analytic method for calculation of the optimum circuit parameters for bandwidth expansion of the ceramic ultrasonic transmitter is described, together with experimental data proving the viability of the method. A low cost wideband ultrasonic receiver array is also presented. The results of the first characterization of MEMs microphones in the ultrasonic band and their use in a sensor array for ultrasonic Array Signal Processing applications is also presented. The paper presents examples of prototype transducer performance in ultrasonic indoor applications.**

***Index Terms*—ultrasonic, array signal processing, piezoelectric, mems**

I. INTRODUCTION

Ultrasonic technology has been increasing in importance in recent years. It has been shown to be effective for indoor location [1], [2], [3], [4], non-destructive studies [5], [6], [7] and medical applications [8], [9]. The demand for improved performance in these applications has created new requirements that are difficult to fulfill using common narrowband ultrasonic transducers. Most ultrasonic transducers have a very narrowband response, which makes them unsuited to broadband applications. In recent years, broadband ultrasonic transducers have been developed using PVDF transducers [10], [11]. However, these need a high voltage supply and do not provide good range, which makes them unsuitable for mobile and low power applications. Other researchers have proposed the use of EMFI transducers, which are not commercially available [12], [13].

This work presents a low cost, low power, wideband ultrasonic transmitter and receiver pair suitable for mobile applications. The designs use commercially available components, reducing production costs. The transmitter and receiver do not need a high polarization voltage (+/- 15 V for the transmitter, +5 V for the receiver) so they can be used in mobile devices and other low power applications. Previously, bandwidth enhancement in piezoceramic applications has been done by modifying the transducer fabrication process, for example by adding new ceramic layers to the transducer or modifying the existing ones [14], [6], [15]. In this work, an electronic circuit for ceramic transducer bandwidth modification is described. The circuit allows for bandwidth increase by adding a resistor and an inductance in parallel with the transducer. An analytic method is described for optimal design of the circuit. A low cost, MEMs based ultrasonic sensor array is also described. To the authors' knowledge , it is the first MEMs microphone array proposed for ultrasonic array application. The small size of the MEMs sensors make them a very good solution for ultrasonic arrays where the distance between sensors usually must be less than 6-7 mm.

This paper is structured as follows: Section II presents a review of ultrasonic technologies, focusing on their advantages and limitations for wideband, low cost and low power applications. Section III explains in detail the piezoelectric technology that was used for this paper. Section IV presents the bandwidth modification procedure used to increase the transducer bandwidth. Section V explains the benefits of MEMs technology for small and compact applications as well as the special requirements of ultrasonic arrays. Section VI presents the method used for transducer characterization, and Section VII presents the results of the prototype characterization study and bandwidth modification experiments and also examples of signal exchange. Section VIII concludes the work.

II. ULTRASONIC TRANSDUCER'S TECHNOLOGY

This section presents a brief overview of the technologies commonly used in ultrasonic applications, such as piezoceramics and composite materials, PVDF, EMFi and CMUTs. It is not within the scope of this section to give the reader deep background theory on the physics of each technology. However, this section does provide an overview of the applications for which they are used, as well as their advantages and limitations, focusing on their application in wideband, low cost and low power systems.

A. Piezoelectric Transducers

Piezoelectric ultrasonic transducers are typically zirconate titanate polymer or composite materials [6]. Typical characteristics of piezoceramic transducers are their high electrical to mechanical efficiency, narrow bandwidth, high impedance and range of possibilities for characteristic modification in production. They are very cost effective for large scale production. Due to their narrow bandwidth (usually 1-3 kHz)

they are not suitable for broadband applications. Also, their high impedance, much greater than air impedance, reduces the maximum Sound Pressure Level (SPL) achieveable, which decreases the maximum signalling range for a given Signal to Noise Ratio (SNR). Other advantages are their easy electronic polarization and small voltage supply.

They have been widely used in indoor location applications, such as the Cricket [2] and BATs [3] systems. These systems use sinusoidal pulses, which give poor performance in reverberant scenarios.

Previous work on bandwidth modification for piezoelectric transducers has focused on finding new piezoelectric materials that provide better properties, such as broader bandwidth response and matched acoustic impedance, [16], [14], [17]. Other work, presented in [15] and [5], presents piezoelectric transducers with a double resonance peak for harmonic imaging, which increases bandwidth and the resolution of imaging applications.

B. PVDF Transducers

Polyvinylidene fluoride (PVDF) was patented by Ford and Hanford and assigned to Pennwalt Corporation (Philadelphia, PA) in 1948 [18]. There has been a great deal of development work on ultrasonic devices that take advantage of the inherent properties of piezoelectric polymers, that is their relatively good acoustic impedance match to water and tissue, their flexible form and availability in large sheets, their broadband acoustic performance, and their ability to be dissolved and coated onto various substrates.

A number of papers have developed theory for building transducers based on PVDF materials [19], [10] and [20]. In addition, several papers have been presented studying the acoustic and electric characteristics of PVDF transducers [11], [21].

Because of the difficulty in creating an efficient PVDF transducer, there are few applications that make use of PVDF materials. Recently, the commercial availability of PVDF cylindrical transducers, such as the US40KT-01 transducer from MSI [22], has increased the number of applications that exploit this material. For example, the authors of [23] use the MSI transducer to improve object position and contour estimation in outdoor environments. Also, the authors of [4] use the transducer to improve the coverage of an indoor location system. However, the mechanical setup necessary to use a PVDF transducer due to the PVDF films' length variation, make it difficult to use in custom acoustic applications. Also, the high polarization voltage that they need, means that they are not the best option for low power applications. The maximum range that transducers based on PVDF can achieve is comparable to the range provided by piezoelectric transducers, having a mean SPL of 110 dB [22].

C. EMFi Transducers

This low cost thin film is a microporous polypropylene foam with high resistivity and permanent charge due to being polarized by the corona method. The resultant inner air voids act as dipoles which make it particularly sensitive to forces normal to its surface. When glued to a rigid substrate and excited by an external voltage, EMFi can be used as an actuator, operating in thickness mode without the influence of the substrate geometry [24], [25]. EMFi has been used to build acoustic transducers, such as physiological sensors [26], keyboards [9], force position sensors [27], etc. The usable frequency range of EMFi film for air applications begins at audible frequencies and extends up to its measured resonance frequency (300 kHz).

Besides its good characteristics, the necessary voltage supply to work, around 110Vpp [24], makes EMFi materials suitable only for fixed devices, for which power consumption is not a mayor issue. However, even for these applications, power can be an issue if a high density of transducers is needed. These high voltages cannot be achieved by mobile devices, which usually require low power consumption for long battery life.

There are no commercially available EMFi based transducers. EMFi films are available, so using an EMFi transducer requires transducer prototyping using a film [28], [29].

D. CMUTs Transducers

Recently, Micro-Electro-Mechanical systems (MEMs), or more specifically, capacitive MEMs ultrasonic transducers (CMUTs) have emerged as an alternative technology offering advantages such as wide bandwidth, ease of fabricating large arrays, and potential for integration with electronics. Sensors, actuators and signal processing components can be integrated into miniaturized smart systems, capable of performing tasks which previously needed the use of a whole range of processes and complex equipment [30], [31]. MEMS technology has demonstrated its economic strength in batch fabrication of large volumes of more or less identical devices [32].

CMUTs are fabricated using standard silicon Integrated Circuit (IC) fabrication technology [33]. This technology makes it possible to create large arrays using simple photolithography. Two-dimensional CMUT arrays with as many as 128x128 elements have already been successfully fabricated and characterized [34]. Individual electrical connections to transducer elements are provided by through-wafer interconnects.

Another enabling feature, inherent to CMUT technology, is its wide bandwidth. A wideband transducer does not simply increase resolution, it also enables the design of new applications and tools. CMUTs are promising for high-frequency applications, such as intravascular ultrasound imaging, in which high-frequency operations using miniature probes are vital. CMUTs operating at frequencies as high as 60 MHz have been fabricated and tested successfully.

MEMs ultrasonic transducers are commercially available e.g. SPM0204 from KnowlesAcoustics [35]. They provide good sensitivity as well as a nearly flat response between 10 and 70 kHz. Their size, 4.72x3.76x1.15 mm makes them useful for compact ultrasonic applications.

E. Summary

In this work piezoelectric transducers were used as transmitters and MEMs sensors as receivers. Because of the advantages

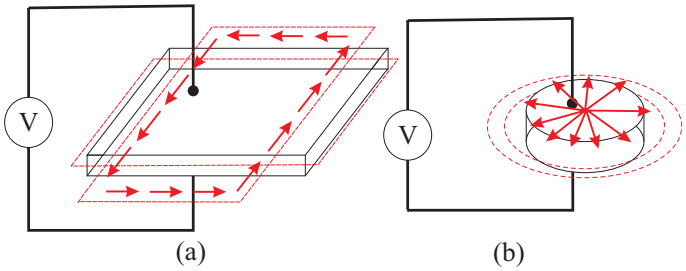

Fig. 1. Resonant Modes in Piezoelectric Transducers: (a) Thickness-Mode; (b) Planar-Mode

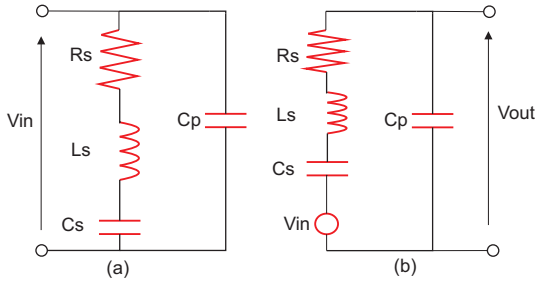

Fig. 2. Piezoelectric Electric Equivalent Circuit. (a) Transmitter; (b) Receiver

presented in Section II-A, high SPL, low complexity electronics and low voltage supply, piezoelectric transducers are a very good option for low power applications. However, because of their resonance characteristics, a bandwidth modification procedure is proposed herein in order to improve performance by enabling wideband signalling. MEMs sensors were chosen because their small size, making them suitable for array processing applications in which several sensors have to be placed with a small physical separation. Also, their good frequency response in the ultrasonic bandwidth, high sensitivity and low supply voltage make them a good choice for implementation in an wideband ultrasonic mobile device.

III. PIEZOELECTRIC TRANSDUCERS

Piezoelectric transducers use a mechanical phenomenon called piezoelectricity, which is a lineal phenomenon that converts the mechanical tension in the material to an induced voltage and vice versa. This phenomenon makes the piezoelectric material vibrate depending on the applied voltage. There are two main resonance modes [6]: planar and thickness. Planar-Mode Resonance, which produces radial vibrations, produces signals with high frequency, usually greater than 1 MHz as is shown in Figure 1 (b). Thickness-Mode Resonance, which produces longitudinal waves, provides signals with small frequency, usually smaller than 1 MHz, as is shown in Figure 1 (a). There are other spurious resonances modes, such as Lateral-Mode Resonances, which are out of the scope of this paper, but are explained in [6].

Piezoceramic transducers are usually made from polycrystal materials. The piezoelectric properties of these crystals are obtained by applying a high voltage to them (usually several kV/mm) during the production process, which orients the dipoles in the direction necessary to provide the desired piezoelectric properties. A number of publications have described research work on piezoelectric-composite materials for low frequency applications (<40 kHz) [36], [37], [38]. Higher frequencies are used for medical diagnostic and nondestructive evaluation (1-10 MHz).

There have been previous work done on bandwidth modification for piezoelectric transducers. It has been focused on finding new piezoelectric materials that could provide better properties, such as broader bandwidth and matched acoustic impedance, as the work presented in [16], [14], [17]. Their results provides slight improvements, but not enough to call the transducers made with their research "broadband". Other work , presented in [15] and [5] are focused on increasing the bandwith of transducers by modifying the materials of the transducers in order to gain a double resonance peak for harmonic imaging, which increases bandwidth and the resolution of imaging applications. But these procedures are difficult to replicate and they do not provide a great bandwidth improvement. The proposed method does not modify the internal structure of the transducer but adding passive components that are easy to replicate and provide a wide bandwidth response.

One of the greatest problems in using piezoceramic transducers in air is that the transducer and medium impedance are badly matched. The transducer impedance determines the Q factor, which determines the bandwidth of the transducer. This mismatch means that the coupling of the acoustic energy at the transducer-load interface is very poor. Also, the high Q (narrow bandwidth) causes a slow pulse-rise time and prolonged ring-down, which reduces the resolution in ranging applications.

Typical bandwidth increasing procedures [39] are based on mechanically damping the piezoelectric element with a well-matched medium which reduces the element's sensitivity, or on using an of impedance matching layer of $\lambda/4$ in thickness and impedance equal to the geometric mean of the transducer-load impedance.

IV. PIEZOELECTRIC BANDWIDTH MODIFICATION

A piezoelectric transducer can be modeled using an equivalent electronic representation. Several models have been proposed [40], [41], [42]. A simplified but efficient representation, i.e. one that represents the device's performance with an acceptable error, can be found in [40] and is shown in Figure 2. This equivalent circuit is called a *Manson circuit*.

The series and parallel resonance frequencies of the circuits presented in Figure 2, both transmitter and receiver, are given by:

$$f_s = \frac{1}{2\pi\sqrt{L_s C_s}} \tag{1}$$

$$f_p = \frac{1}{2\pi\sqrt{L_s \frac{C_s C_p}{C_s + C_p}}} \tag{2}$$

The piezoelectric resonant frequency is either the series resonance frequency f_s, the minimum impedance frequency f_m or the smallest of f_s and f_m, called f_{rr} . Usually, the

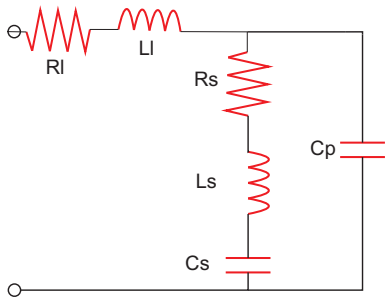

Fig. 3. Compensated Piezoelectric Electric Equivalent Circuit

three of these are nearly the same, so f_m is taken to be the resonant frequency, f_r, because it can be easily calculated.

The acoustic power transmitted by the transducer is proportional to the power dissipated in the resistor shown in Figure 2 (a). Using the Laplace transform, the current through the resistor R_s is defined as follows:

$$I_M = \frac{V_{in}}{L_s s + \frac{1}{C_s s} + R_s} \tag{3}$$

$$\frac{I_M}{V_{in}} = \frac{\frac{1}{L_s} s}{s^2 + \frac{R_s}{L_s} s + \frac{1}{L_s C_s}} \tag{4}$$

By defining w_n and ξ as follows:

$$w_n^2 = \frac{1}{L_s C_s} \quad \xi = \frac{R_s}{2}\sqrt{\frac{C_s}{L_s}} \tag{5}$$

Equation 4 can be expressed as:

$$Y(s) = \frac{\frac{1}{L_s} s}{s^2 + 2\xi w_n + w_n^2} \tag{6}$$

which has the same structure as a band-pass filter, with w_n as the filter's resonant frequency and ξ as a factor related to the filter's bandwidth.

If an inductance and a resistor are added to the circuit, as shown in Figure 3, a second peak appears in the frequency response. If this second peak is correctly chosen, the transducer's bandwidth is increased, but its sensitivity is slightly reduced. The Laplace response $Y_1(s)$ is then:

$$\left(Rs + L_s s + \frac{1}{C_s s}\right) \parallel \frac{1}{C_p s} = X_s \parallel X_p \tag{7}$$

$$X_s \parallel X_p = \frac{L_s s + R_s + 1/C_s s}{C_p L_s s^2 + C_p R_s s + \frac{C_s + C_p}{C_s}} \tag{8}$$

$$Y_1(s) = \frac{X_s \parallel X_p}{X_s \parallel X_p + R_L + L_L s} \cdot \frac{1}{R_s + L_s s + \frac{1}{C_s s}} \tag{9}$$

where $\parallel$ is the parallel equivalent impedance, X_s is the equivalent series impedance of R_s, L_s and C_s and X_p is the equivalent impedance of C_p.

Figure 4 shows the effect of inductance and resistor values on the compensated frequency response. The thick black line represents the unmodified frequency response. The thin lines represent the modified frequency responses. As can be seen,

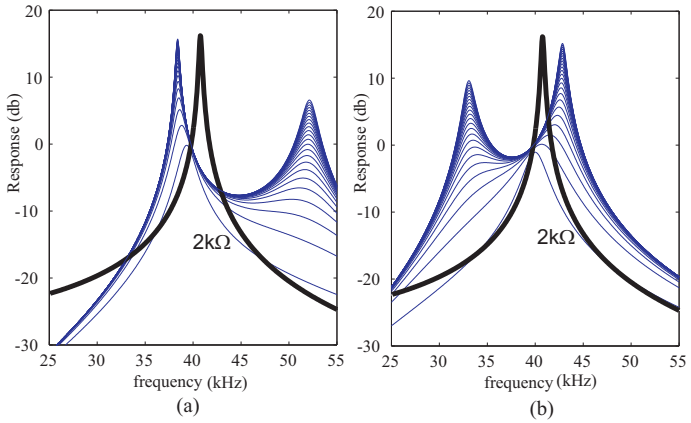

Fig. 4. Frequency Response of compensated (thin) and non-compensated (thick) transducer for R=100Ω-2kΩ: (a) Lc=5mH; (b) Lc=10mH

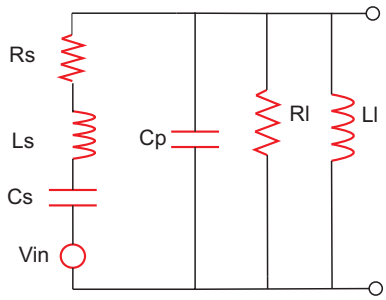

Fig. 5. Compensated Receiver Piezoelectric Electric Equivalent Circuit

the inductance controls the frequency of the secondary peak, and the resistance controls the amplitude of the peaks.

This procedure can be applied to the receiver by adding the inductance and resistor in parallel to the equivalent circuit as shown in Figure 5. This provides similar results as for the transmitter.

C_p is calculated using the formula in Eq. 10, which makes use of the transducer impedance Z at a given frequency f.

$$C_p = \frac{1}{|Z| 2\pi f} \tag{10}$$

In order to obtain the impedance of the transducer for different frequencies, the circuit shown in Figure 8 is used and the voltage V_m is calculated. As the impedance of R is known, the current can be easily obtained, and the voltage in the transducer can be calculated as $V_{tx} = V_{in} - V_m$.

Once the parallel capacitance C_p is obtained, the equivalent series resistance is calculated as:

$$R_s = \frac{|Z|}{\sqrt{1 - (|Z| C_p 2\pi f_m)^2}} \tag{11}$$

Use is made of C_p, and the impedance at the resonant frequency to determine R_s. The resonant frequency is the one with maximum impedance, which means that voltage is maximum.

$$f_m = \frac{1}{2\pi\sqrt{C_s L_s}} \tag{12}$$

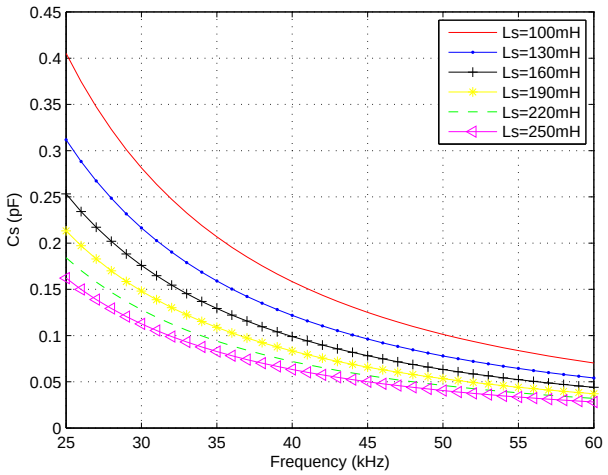

Fig. 6. Parametric Cs and Ls values for different frequencies

L_s and C_s can be calculated using the relation presented in Eq. 12, which relates them to the resonant frequency. Parametric plots can be seen in Figure 6 between 25 and 60 kHz. They were created for various values of C_s, L_s and frequencies.

V. CMUTs TECHNOLOGY IN ARRAY SIGNAL PROCESSING

Array Signal Processing (ASP) is used in many applications. Beamforming techniques have been used to improve system performance [43] and to provide extra information [44], [45]. The study presented in [46] and [47] shows the benefits obtained in mobile communications by using an adaptive antenna with beamforming techniques. In [48], location is estimated in Wireless Sensor Networks by computing the Angle of Arrival (AoA) of the exchanged signals.

The basis of any Array Signal Processing stems from assuming a signal arrives at an array of M sensors. The signal arrives with direction (ϕ, θ) where ϕ is the source elevation and θ is the source azimuth. The received signal at the center of the array is defined as:

$$x_{ref}(t) = a(t)\exp(jw_0 t) \tag{13}$$

where $a(t)$ is the complex-envelope of the signal. The signal received at the sensor m is defined as:

$$x_m(t) = a(t)\exp(jw_0 t)\exp(j\Theta_m) \tag{14}$$

where Θ_m is the phase delay between the signal at sensor m and the central sensor.

Let us assume that a set of N_S signals arrive at an array, with direction $[\phi_n, \theta_n], n = 1, ...N_S$. The received signal at each sensor at an instant n is called a *snapshot* and is defined as [45]:

$$\underline{X}_n = \underline{\underline{A}}\underline{S} + \underline{w}_n \tag{15}$$

$$\underline{S} = \begin{bmatrix} S_1(n) \\ S_2(n) \\ \vdots \\ S_{NS}(n) \end{bmatrix} \tag{16}$$

$$\underline{\underline{A}} = [\underline{a}_1(\varsigma_1, \phi_1), \underline{a}_2(\varsigma_2, \phi_2) \cdots, \underline{a}_{NS}(\varsigma_{NS}, \phi_{NS})] \tag{17}$$

where $S_i(n)$ is the complex envelope of each of the N_S signals at time n, $\underline{\underline{A}}$ is a matrix containing the AoA of each signal, and $\underline{w}_n$ is independent White Gaussian noise at each sensor. The snapshot is basically, the sum of contributions of a set of sources plus noise.

Most AoA estimators operate on the Covariance Matrix of the received snapshots [49], [50], [51], [52]. The covariance matrix R is ideally obtained by calculating the correlations between the sensors and placing the results in a MxM matrix, where M is the number of sensors in the array.

$$\underline{\underline{R}} = E\left[X_n \cdot X_n^H\right] \tag{18}$$

In practical applications, the number of observations is limited to a number of snapshots N_{snap}. In this case, the covariance matrix is estimated according to:

$$\underline{\underline{\hat{R}}} = \frac{1}{N}\sum_{q=0}^{N_{snap}-1} X_{n-q}X_{n-q}^H \tag{19}$$

ASP based AoA estimators are based on the phase difference between a signal arriving at different sensors with a known waveform. The maximum unambiguous phase difference between two sensors is $\pm\pi$. If d is the distance between two sensors, then we must have $d \leq \frac{\pi c}{2\pi f} = \frac{\lambda}{2}$ in order to provide a phase difference of less than or equal to $\pm\pi$. As can be seen in Table I, for low frequency ultrasonic signals, up to 45 kHz, the maximum distance between sensors is 3.81 mm. For greater frequencies, the distance decreases, to 1.8 mm for a 95 kHz signal.

An scheme of an Array Signal Processing is shown in Figure 7. A set of N sensors receive a signal that is processed by a signal processing circuit at each sensor. Finally, those signals are combined to provide the output.

TABLE I
MAXIMUM DISTANCE BETWEEN SENSORS FOR C=343 M/S

Frequency (kHz)	Wavelength (mm)	Maximum Distance (mm)
25	13.72	6.86
35	9.80	4.90
45	7.62	3.81
65	5.27	2.64
95	3.61	1.80

Commonly, ultrasonic receivers have a diameter greater than that which would allow construction of an ultrasonic array with sensor separation of around 7 mm. If the maximum sensor separation requirement is not met, the beamforming or Angle of Arrival estimation process becomes ambiguous. Hence, the system is unable to correctly estimate the phase delays, providing multiple possible solutions rather than a single robust

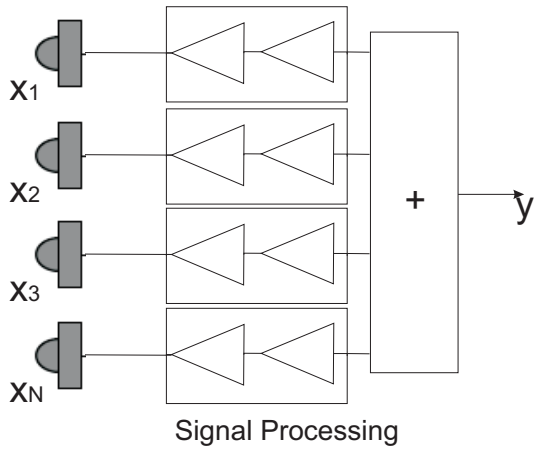

Fig. 7. Array Signal Processing Scheme

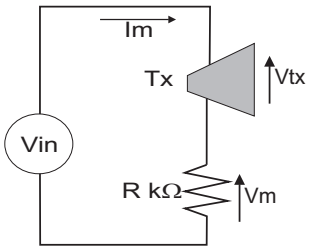

Fig. 8. Transducer Test Circuit

solution. Using CMUT sensors in ultrasonic array applications allows smaller array sizes which can support Array Signal Processing algorithms without causing ambiguities.

VI. METHOD

This section describes the method used to characterize the transmitters and modify their bandwidth, as well as the tests performed on the receiver array. The first step in the modification process is obtaining the equivalent circuit parameters. These parameters are calculated based on the voltage and impedance of the transducer at a given frequency. The circuit shown in Figure 8 was built in order to obtain these measurements. Four transducers were used in order to provide results for transducers with different resonant frequency. The transducers chosen were PROWAVE [53], models: 250ST180 (25kHz), 328ET250 (32kHz), 400ET180 (40kHz) and 400EP900 (50kHz).

The procedure presented in Section IV was applied. Finding the elements in the equivalent circuit, estimating the inductance and resistance, adding them in series to the transducer and obtaining the frequency response. The test circuit, shown in Figure 8, was connected to a signal generator applying a sinusoidal wave of 15 Vpp. The transducer was connected, and a resistor R in series, whose value was 1.014 kΩ. Frequency response characterization was done by placing the transmitter and receiver face-to-face and sending sinusoidal pulses between them from 10 kHz to 50 kHz, with a separation of 100 Hz. For each sinusoid, the mean amplitude was calculated and used as data point in the presented plots. The results were corrected to allow for the receiver response. The receiver frequency response of the *SPM0204* sensor is given in the datasheet, Figure. 10.

The design process has an optimization criterion of maximizing the bandwidth at -15 dB. The transducer parameters were applied to an optimization procedure in order to find the inductance value that provides two resonance peaks equally separated from the original narrow peak. Once the inductance value has been chosen, so as to provide a modified frequency response centered on the original resonance, an iterative procedure was applied, to search for the resistance providing maximum bandwidth at -15 db, ideally with the smallest resonance peaks variation, in order to ensure small variations in the frequency response around the usable bandwidth.

For the receiver array, the first element characterized was the mutual coupling between channels. When only one channel is on, the signal received from all other channels was measured. The mean energy was calculated in order to obtain the mutual coupling matrix [45], [43]. This matrix provides information on the mutual coupling between channels. The channel mismatch in amplitude and continuous component was also measured, in order to assess the variation between the elements in the array.

VII. RESULTS

TABLE II
TRANSDUCER VOLTAGE FOR DIFFERENT FREQUENCY EXCITATIONS (VOLTS)

Freq (kHz)	**Vtx(25kHz)** (Vpp)	**Vtx(32kHz)** (Vpp)	**Vtx(40kHz)** (Vpp)	**Vtx(48kHz)** (Vpp)
20.0	6.70	7.00	7.20	7.00
25.0	5.20	6.70	6.44	6.40
27.5	**8.68**	6.30	6.30	6.20
30.0	7.60	5.80	6.00	5.90
32.5	6.45	4.80	5.55	5.60
35.0	5.95	**9.02**	5.00	5.20
40.0	4.00	6.00	3.20	4.50
42.5	6.80	5.50	**8.40**	4.40
45.0	6.80	5.20	5.70	4.20
47.5	5.70	4.80	5.20	3.90
50.0	5.20	4.60	4.80	3.60
55.0	4.50	4.20	4.40	**8.10**
60.0	4.05	3.60	3.85	7.00

Tables II and III show the results obtained when measuring voltage and impedance for the transducers using the circuit presented in Figure 8, with $R = 1.014k\Omega$. Voltage was measured at the resonant frequencies of each transducer.

Table IV presents the equivalent circuit components for all of the transducers, obtained using the process explained in Section IV and the data from Tables II and III. Figure 9 shows the estimated compensated frequency response for the transducers modeled with the components listed in Table IV. The effect of the compensation process on all of the transducers' responses can be seen in Figure 9. The circuit

TABLE III
TRANSDUCER IMPEDANCE MEASUREMENTS FOR DIFFERENT FREQUENCY EXCITATIONS

Freq (kHz)	**Z(25kHz)** (kΩ)	**Z(32kHz)** (kΩ)	**Z(40kkHz)** (kΩ)	**Z(48kkHz)** (kΩ)
20.0	2.06	2.37	2.26	2.37
25.0	1.10	2.06	1.83	1.80
27.5	6.67	1.73	1.73	1.65
30.0	3.21	1.40	1.52	1.46
32.5	1.84	0.94	1.24	1.29
35.0	1.49	9.13	1.01	1.10
40.0	0.68	1.52	0.48	0.83
42.5	1.02	1.24	5.32	0.80
45.0	2.16	1.10	1.34	0.73
47.5	1.35	0.94	1.10	0.65
50.0	1.10	0.86	0.94	0.57
55.0	0.83	0.73	0.80	4.06
60.0	0.69	0.57	0.63	2.37

TABLE IV
TRANSDUCER EQUIVALENT CIRCUIT COMPONENTS

Tx Model	C_p (nF)	R_s (kΩ)	C_s (nF)	L_s (mH)
250ST180	3.84	2.65	0.25	160
328ET250	4.65	2.08	0.15	160
400ET180	3.05	1.95	0.10	160
400EP900	3.36	2.77	0.07	160

provides a significant improvement in bandwidth, achieving a bandwidth of 10-15 kHz, depending on the transducer.

Figure 10 shows the results of the modifications for the 4 real transducers. It can be seen that the measurements match the estimates very well. It can be seen that the second peak appears for all transducers, increasing the bandwidth significantly.

Figure 12 shows the antenna array built using the MEMs sensors. The separation between sensors is 4.71 mm, allowing a maximum frequency of 40kHz without ambiguity. The size makes it suitable for compact applications, as can be seen in Figure 12. The voltage supply necessary for the sensors is 3.3 Volts. and the current consumption varies between 0.1 to 0.25 mA as is stated in the datasheet [35]. As can be seen, it is a very good option for low power applications.

TABLE V
RECEIVER CHANNELS' MUTUAL COUPLING INDEX

	CHr (mV)	**CH1** (mV)	**CH2** (mV)	**CH3** (mV)	**CH4** (mV)	**CH5** (mV)	**CH6** (mV)
CHr	51.0	1.04	1.34	1.14	1.26	0.95	0.92
CH1	1.96	49.0	2.18	1.19	1.50	1.11	1.25
CH2	0.83	0.63	18.5	1.05	0.24	0.22	0.56
CH3	1.04	0.87	1.24	24.3	1.16	0.25	2.05
CH4	1.05	1.21	0.83	1.25	15.8	1.30	1.20
CH5	0.95	1.18	0.94	0.99	3.01	37.6	0.93
CH6	1.22	1.17	1.29	0.64	1.29	1.52	50.9

Table V gives the voltage received in all the channels when only one sensor is receiving signals. With the information in this table, the mutual coupling matrix was computed, as was explained in Eq. 20. The contribution to one channel from the others is very small, allowing for precise and robust Array Signal Processing algorithms.

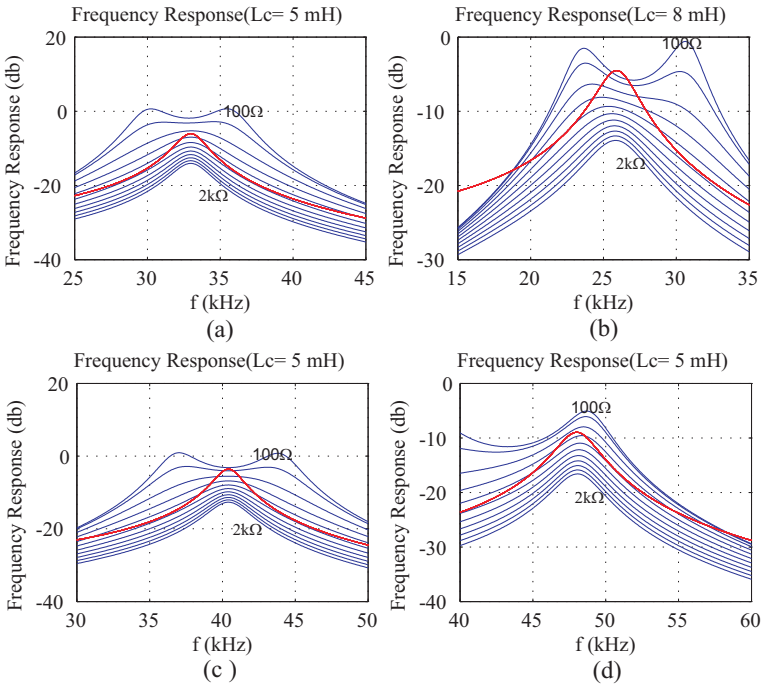

Fig. 9. Estimated modified frequency responses for transducer, RL from 100Ω to 2kΩ : (a) 250ST180; (b) 328ET250 (c) 400ET180 (d) 400EP900

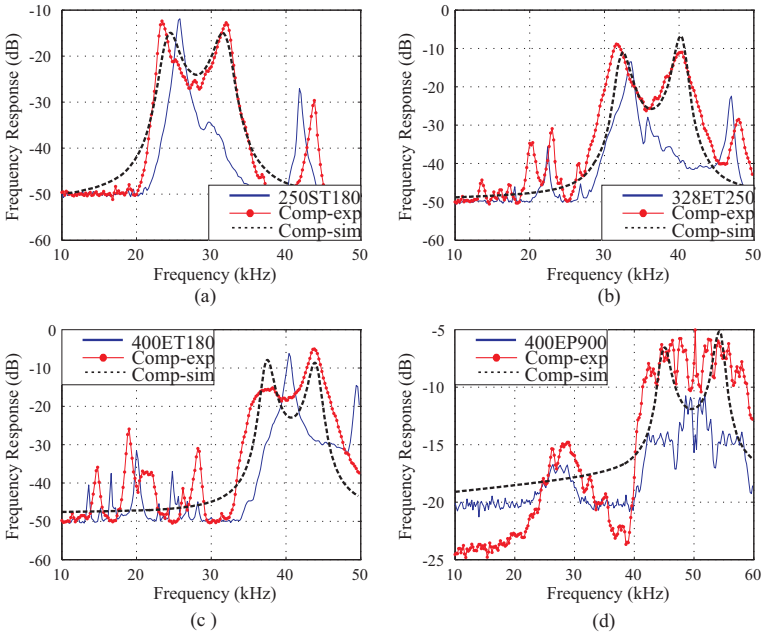

Fig. 10. Measured modified frequency responses for transducer, line - ideal, dot - simulated, points - experimental: (a) 250ST180; (b) 328ET250 (c) 400ET180 (d) 400EP900

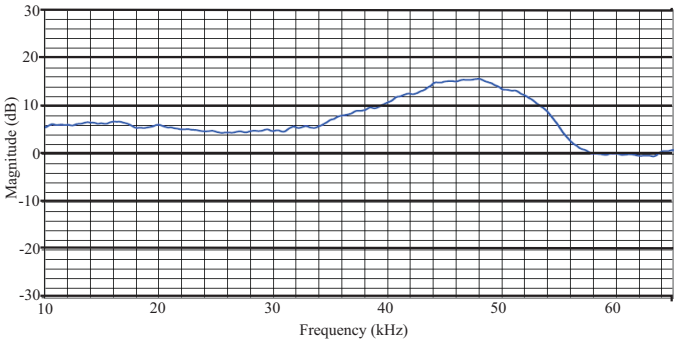

Fig. 11. Receiver Frequency Response [35]

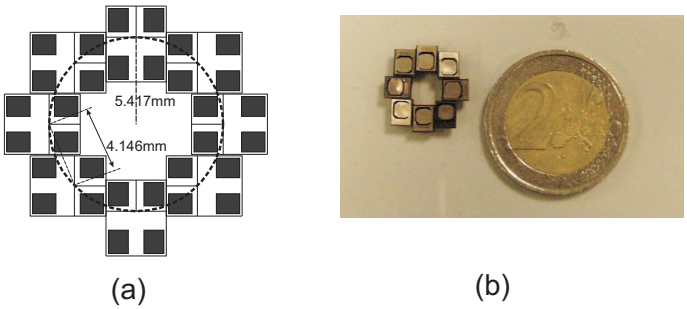

Fig. 12. Antenna array: (a) footprint; (b) picture

$$G|_{40kHz} = \begin{bmatrix} 1 & 0.04 & 0.02 & 0.03 & 0.02 & 0.03 \\ 0.03 & 1 & 0.06 & 0.01 & 0.01 & 0.03 \\ 0.04 & 0.05 & 1 & 0.05 & 0.01 & 0.08 \\ 0.08 & 0.05 & 0.08 & 1 & 0.08 & 0.08 \\ 0.03 & 0.02 & 0.03 & 0.08 & 1 & 0.02 \\ 0.02 & 0.03 & 0.01 & 0.03 & 0.03 & 1 \end{bmatrix} \quad (20)$$

TABLE VI
CONTINUOUS COMPONENT AND AMPLITUDE MISMATCH BETWEEN CHANNELS

Channel	Amplitude (V)	Amp. mistmach(%)	Continuous C.(V)
CHr	3.67	0.00	0.00
CH1	3.75	2.40	0.01
CH2	3.66	0.22	0.00
CH3	3.50	4.52	0.01
CH4	3.75	2.06	0.01
CH5	3.69	0.67	0.01
CH6	3.59	2.04	0.02

Table VI shows the mismatch between channels. The first column is the amplitude of the received signal at each channel. The second column is the deviation of each channel with respect the reference channel CHr in %. The third column is the deviation in the continuous component with respect the reference channel, in Volts. As can be seen, the mismatch is small enough so as to be discarded.

Table VII shows the SNR values obtained in the tested room between the transmitter and receiver proposed. A sinusoidal of 40 kHz was sent, with an amplitude of 14 Vpp. The receiver was supplied by a 3.6 volts battery, and an amplifier of 20. The mean Vpp was calculated for the background noise and signal.

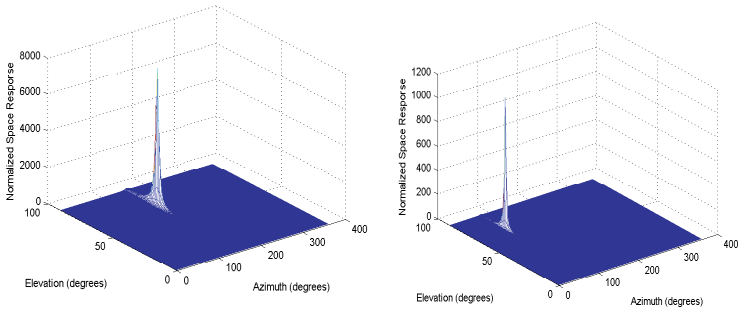

Fig. 13. Angle of Arrival estimation using MEM array prototype

TABLE VII
SNR VALUES IN TESTED ROOM

Distance (meters)	SNR (dB)
1.12	33.40
1.67	30.45
2.60	25.45
3.57	20.12

As can be seen, it provides very good SNR in the indoor ranges measured for a low transmitter and receiver polarization.

Two examples of Angle of Arrival estimation using the array are shown in Figure 13. The clear peaks indicate high accuracy, which is due to the good mutual coupling characteristics and small channel missmatch in the sensors. The higher and narrower the peak, the more accurate and robust the estimates.

VIII. CONCLUSIONS

In this paper, a review of ultrasonic in-air technologies was described. The review focused on low cost, low power wideband applications, where it was shown that there is no existing optimal technology. A modification process was presented, which allows a significant increase in piezoelectric transducer bandwidth by adding 2 passive components, an inductor and a resistor. The theory used was explained and validated by simulations and experimental results.

Also, the paper details how MEMs technology can be used for Array Signal Processing applications in the ultrasonic band. The antenna schematics have been presented, as well as the antenna characterization.

This combination of wideband transmitter and receiver array opens up to possibilities of novel commercial applications such as novel location-orientation systems, new health-care sensing devices or human-computer communication devices.

ACKNOWLEDGMENT

The work presented in this paper was supported by a research grant from Science Foundation Ireland.

REFERENCES

[1] J. Hightower and G. Borriello, "Location systems for ubiquitous computing," *COMPUTER*, pp. 57–66, 2001.

[2] N. Priyantha, A. Chakraborty, and H. Balakrishnan, "The cricket location-support system," in *Proceedings of the 6th annual international conference on Mobile computing and networking*. ACM Press New York, NY, USA, 2000, pp. 32–43.

[3] A. Harter, A. Hopper, P. Steggles, A. Ward, and P. Webster, "The anatomy of a context-aware application," *Wireless Networks*, vol. 8, no. 2, pp. 187–197, 2002.

[4] J. Villadangos, J. Urena, M. Mazo, A. Hernandez, C. De Marziani, A. Jimenez, and F. Alvarez, "Improvement of cover area in ultrasonic local positioning system using cylindrical pvdf transducer," in *Industrial Electronics, 2007. ISIE 2007. IEEE International Symposium on*, 2007, pp. 1473–1477.

[5] S. Takeuchi, M. Al Zaabi, T. Sato, and N. Kawashima, "Study on ultrasound transducer with double peak type frequency characteristics for sub-harmonic imaging," in *Ultrasonics Symposium, 2002. Proceedings. 2002 IEEE*, vol. 2, 2002.

[6] T. GURURAJA, W. SCHULZE, L. CROSS, R. NEWNHAM, B. AULD, and Y. WANG, "Piezoelectric composite materials for ultrasonic transducer applications. i: resonant modes of vibration of pzt rod-polymer composites," *IEEE transactions on sonics and ultrasonics*, vol. 32, no. 4, pp. 481–498, 1985.

[7] O. Oralkan, A. Ergun, J. Johnson, M. Karaman, U. Demirci, K. Kaviani, T. Lee, and B. Khuri-Yakub, "Capacitive micromachined ultrasonic transducers: next-generation arrays for acoustic imaging?" *Ultrasonics, Ferroelectrics and Frequency Control, IEEE Transactions on*, vol. 49, no. 11, pp. 1596–1610, 2002.

[8] S. Karki and J. Lekkala, "Film-type transducer materials pvdf and emfi in the measurement of heart and respiration rates," in *Engineering in Medicine and Biology Society, 2008. EMBS 2008. 30th Annual International Conference of the IEEE*, 2008, pp. 530–533.

[9] H. Sorvoja, V. Kokko, R. Myllyla, and J. Miettinen, "Use of emfi as a blood pressure pulse transducer," *Instrumentation and Measurement, IEEE Transactions on*, vol. 54, no. 6, pp. 2505–2512, 2005.

[10] A. Fiorillo, "Design and characterization of a pvdf ultrasonic range sensor," *Ultrasonics, Ferroelectrics and Frequency Control, IEEE Transactions on*, vol. 39, no. 6, pp. 688–692, 1992.

[11] P. Bloomfield, W. Lo, and P. Lewin, "Experimental study of the acoustical properties of polymers utilized to construct pvdf ultrasonic transducers and the acousto-electric properties of pvdf and p (vdf/trfe) films," *Ultrasonics, Ferroelectrics and Frequency Control, IEEE Transactions on*, vol. 47, no. 6, pp. 1397–1405, 2000.

[12] M. Hazas and A. Ward, "A novel broadband ultrasonic location system," *LECTURE NOTES IN COMPUTER SCIENCE*, pp. 264–280, 2002.

[13] L. Barna, M. Koivuluoma, M. Hasu, J. Tuppurainen, and A. Varri, "The use of electromechanical film (emfi) sensors in building a robust touch-sensitive tablet-like interface," *Sensors Journal, IEEE*, vol. 7, no. 1, pp. 74–80, 2007.

[14] A. Cochran, G. Hayward, and V. Murray, "Multilayer piezocomposite ultrasonic transducers operating below 50khz," in *Ultrasonics Symposium, 1999. Proceedings. 1999 IEEE*, vol. 2, 1999.

[15] S. Takeuchi, M. Al Zaabi, T. Sato, and N. Kawashima, "Development of ultrasound transducer with double-peak-type frequency characteristics for harmonic imaging and subharmonic imaging," *Jpn. J. Appl. Phys*, vol. 41, pp. 3619–3623, 2002.

[16] A. Cochran, P. Reynolds, and G. Hayward, "Multilayer piezocomposite transducers for applications of lowfrequency ultrasound," in *Ultrasonics Symposium, 1997. Proceedings., 1997 IEEE*, vol. 2, 1997.

[17] W. Smith, "The role of piezocomposites in ultrasonic transducers," in *Ultrasonics Symposium, 1989. Proceedings., IEEE 1989*, 1989, pp. 755–766.

[18] F. T. H. W.E., "Polyvinylidene fluoride and process for obtaining the same," U.S. Patent 2 435 537, 1948.

[19] L. Brown, "Design considerations for piezoelectric polymer ultrasound transducers," *Ultrasonics, Ferroelectrics and Frequency Control, IEEE Transactions on*, vol. 47, no. 6, pp. 1377–1396, 2000.

[20] M. Toda, "Cylindrical pvdf film transmitters and receivers for air ultrasound," *Ultrasonics, Ferroelectrics and Frequency Control, IEEE Transactions on*, vol. 49, no. 5, pp. 626–634, 2002.

[21] J. Lan, S. Boucher, and R. Tancrell, "Investigation of broadband characteristics of pvdf ultrasonictransducers by finite element modeling and experiments," in *Ultrasonics Symposium, 1999. Proceedings. 1999 IEEE*, vol. 2, 1999.

[22] MSI. Pvdf 40 khz transducer. http://www.ehag.ch/PDF-Files/MSI/40khz-transmitter.pdf.

[23] A. Jimenez and F. Seco, "Precise localisation of archaeological findings with a new ultrasonic 3d positioning sensor," *Sensors & Actuators: A. Physical*, vol. 123, pp. 224–233, 2005.

[24] J. Ealo, A. Jimenez, F. Seco, C. Prieto, J. Roa, F. Ramos, and J. Guevara, "Broadband omnidirectional ultrasonic transducer for air ultrasound based on emfi," in *Ultrasonics Symposium, 2006. IEEE*, 2006, pp. 812–815.

[25] J. Ealo, F. Seco, and A. Jimenez, "Broadband emfi-based transducers for ultrasonic air applications," *Ultrasonics, Ferroelectrics and Frequency Control, IEEE Transactions on*, vol. 55, no. 4, pp. 919–929, 2008.

[26] J. Alametsä, E. Rauhala, E. Huupponen, A. Saastamoinen, A. Värri, A. Joutsen, J. Hasan, and S. Himanen, "Automatic detection of spiking events in emfi sheet during sleep," *Medical Engineering and Physics*, vol. 28, no. 3, pp. 267–275, 2006.

[27] G. Evreinov and R. Raisamo, "One-directional position-sensitive force transducer based on emfi," *Sensors & Actuators: A. Physical*, vol. 123, pp. 204–209, 2005.

[28] S. Karki, M. Kaariainen, and J. Lekkala, "Measurement of heart sounds with emfi transducer," in *Engineering in Medicine and Biology Society, 2007. EMBS 2007. 29th Annual International Conference of the IEEE*, 2007, pp. 1683–1686.

[29] A. Jiménez, Á. Hernández, J. Ureña, M. Pérez, F. Álvarez, C. De Marziani, J. García, and J. Villadangos, "Emfi-based ultrasonic transducer for robotics applications," *Sensors & Actuators: A. Physical*, 2008.

[30] V. Sarihan, J. Wen, G. Li, T. Koschmieder, R. Hooper, R. Shumway, and J. Macdonald, "Designing small footprint, low-cost, high-reliability packages for performance sensitive mems sensors," in *Electronic Components and Technology Conference, 2008. ECTC 2008. 58th*, 2008, pp. 817–818.

[31] M. Schuenemann, K. Jam, V. Grosser, R. Leutenbauer, G. Bauer, W. Schaefer, and H. Reichl, "Mems modular packaging and interfaces," in *Electronic Components and Technology Conference, 2000. 2000 Proceedings. 50th*, 2000, pp. 681–688.

[32] R. Tummala and V. Madisetti, "System on chip or system on package?" *Design & Test of Computers, IEEE*, vol. 16, no. 2, pp. 48–56, 1999.

[33] A. Schubring and Y. Fujita, "Ceramic package solutions for mems sensors," in *Electronic Manufacturing Technology Symposium, 2007. IEMT'07. 32nd IEEE/CPMT International*, 2007, pp. 268–272.

[34] C. Cheng, E. Khuri, and B. Yakub, "An efficient electrical addressing method using through-wafer viasfor two-dimensional ultrasonic arrays," in *Ultrasonics Symposium, 2000 IEEE*, vol. 2, 2000.

[35] K. Acoutics, "Spm0204 mems sensor," *http://www.knowleselectronics.com/*.

[36] K. KLICKER, J. BIGGERS, and R. NEWNHAM, "Composites of pzt and epoxy for hydrostatic transducer applications," *Journal of the American Ceramic Society*, vol. 64, no. 1, pp. 5–9, 1981.

[37] R. Newnham, D. Skinner, L. Cross *et al.*, "Connectivity and piezoelectric-pyroelectric composites," *Mater. Res. Bull*, vol. 13, no. 5, pp. 525–536, 1978.

[38] D. Skinner, R. Newnham, and L. Cross, "Flexible composite transducers," *Mater. Res. Bull*, vol. 13, no. 6, pp. 599–607, 1978.

[39] G. Kossoff, "The effects of backing and matching on the performance of piezoelectric ceramic transducers," *Sonics and Ultrasonics, IEEE Transactions on*, vol. 13, no. 1, pp. 20–30, 1966.

[40] E. Courses and T. Surveys, "An electromechanical representation of a piezoelectric crystal used as a transducer," *Proceedings of the IRE*, vol. 23, no. 10, pp. 1252–1263, 1935.

[41] K. Ymada, J. Sakamura, and K. Nakamura, "Equivalent network analysis of piezoelectrically-graded broadbandultrasound transducers," in *Ultrasonics Symposium, 1999. Proceedings. 1999 IEEE*, vol. 2, 1999.

[42] D. Church and D. Pincock, "Predicting the electrical equivalent of piezoceramic transducers for small acoustic transmitters," *Sonics and Ultrasonics, IEEE Transactions on*, vol. 32, no. 1, pp. 61–64, 1985.

[43] B. Van Veen and K. Buckley, "Beamforming: a versatile approach to spatial filtering," *ASSP Magazine, IEEE [see also IEEE Signal Processing Magazine]*, vol. 5, no. 2, pp. 4–24, 1988.

[44] H. Van Trees, *Optimum Array Processing: Part IV of Detection, Estimation and Modulation Theory*. John Wiley & Sons, 2002.

[45] H. Krim, M. Viberg, and C. MIT, "Two decades of array signal processing research: the parametricapproach," *Signal Processing Magazine, IEEE*, vol. 13, no. 4, pp. 67–94, 1996.

[46] L. Godara, "Application of antenna arrays to mobile communications. ii. beam-forming and direction-of-arrival considerations," *Proceedings of the IEEE*, vol. 85, no. 8, pp. 1195–1245, 1997.

[47] L. Godara, N. Wales, and A. Canberra, "Applications of antenna arrays to mobile communications. i. performance improvement, feasibility, and system considerations," *Proceedings of the IEEE*, vol. 85, no. 7, pp. 1031–1060, 1997.

[48] P. Rong and M. Sichitiu, "Angle of arrival localization for wireless sensor networks," *Sensor and Ad Hoc Communications and Networks, 2006. SECON'06. 2006 3rd Annual IEEE Communications Society on*, vol. 1, 2006.

[49] C. Mathews and M. Zoltowski, "Eigenstructure techniques for 2-d angle estimation with uniformcircular arrays," *Signal Processing, IEEE Transactions on [see also Acoustics, Speech, and Signal Processing, IEEE Transactions on]*, vol. 42, no. 9, pp. 2395–2407, 1994.

[50] D. Ward, Z. Ding, and R. Kennedy, "Broadband doa estimation using frequency invariant beamforming," *Signal Processing, IEEE Transactions on [see also Acoustics, Speech, and Signal Processing, IEEE Transactions on]*, vol. 46, no. 5, pp. 1463–1469, 1998.

[51] B. Ottersten and T. Kailath, "Direction-of-arrival estimation for wide-band signals using theesprit algorithm," *Acoustics, Speech, and Signal Processing [see also IEEE Transactions on Signal Processing], IEEE Transactions on*, vol. 38, no. 2, pp. 317–327, 1990.

[52] S. Kay and S. Marple Jr, "Spectrum analysisa modern perspective," *Proceedings of the IEEE*, vol. 69, no. 11, pp. 1380–1419, 1981.

[53] Prowave, "Piezoelectric ultrasonic transducers," *http://www.prowave.com.tw/*.